Underground Ammunition Storage Magazines: Effects of Loading Density on Dynamic Airblast Flow in Small-Scale Models

by

Charles E. Joachim
Gordon W. McMahon
Christo V. Lunderman
Sharon B. Garner

U.S. Army Engineer Waterways Experiment Station
3909 Halls Ferry Road
Vicksburg, MS 39180-6199

Prepared for:
28th DoD Explosives Safety Seminar
18-20 August 1998
Orlando, Florida

Report Documentation Page

Form Approved
OMB No. 0704-0188

1. REPORT DATE	2. REPORT TYPE	3. DATES COVERED
AUG 1998		**00-00-1998 to 00-00-1998**

4. TITLE AND SUBTITLE	5a. CONTRACT NUMBER
Underground Ammunition Storage Magazines: Effects of Loading Density on Dynamic Airblast Flow in Small-Scale Models	5b. GRANT NUMBER
	5c. PROGRAM ELEMENT NUMBER
6. AUTHOR(S)	5d. PROJECT NUMBER
	5e. TASK NUMBER
	5f. WORK UNIT NUMBER
7. PERFORMING ORGANIZATION NAME(S) AND ADDRESS(ES) **U.S. Army Engineer Waterways Experiment Station,3909 Halls Ferry Road,Vicksburg,MS,39180-6199**	8. PERFORMING ORGANIZATION REPORT NUMBER
9. SPONSORING/MONITORING AGENCY NAME(S) AND ADDRESS(ES)	10. SPONSOR/MONITOR'S ACRONYM(S)
	11. SPONSOR/MONITOR'S REPORT NUMBER(S)

12. DISTRIBUTION/AVAILABILITY STATEMENT
Approved for public release; distribution unlimited

13. SUPPLEMENTARY NOTES
See also ADM001002. Proceedings of the Twenty-Eighth DoD Explosives Safety Seminar Held in Orlando, FL on 18-20 August 1998.

14. ABSTRACT
see report

15. SUBJECT TERMS

16. SECURITY CLASSIFICATION OF:			17. LIMITATION OF ABSTRACT	18. NUMBER OF PAGES	19a. NAME OF RESPONSIBLE PERSON
a. REPORT **unclassified**	b. ABSTRACT **unclassified**	c. THIS PAGE **unclassified**	**Same as Report (SAR)**	**24**	

Underground Ammunition Storage Magazines: Effects of Loading Density on Dynamic Airblast Flow in Small-Scale Models

by

Charles E. Joachim
Gordon W. McMahon
Christo V. Lunderman
Sharon B. Garner

U.S. Army Engineer Waterways Experiment Station
3909 Halls Ferry Road
Vicksburg, MS 39180-6199

ABSTRACT

A series of 1:20-scale model experiments were conducted to investigate the effects of loading density on the dynamic airblast flow parameters produced by spherical charge detonations in a model underground ammunition storage magazine (shotgun design). Total pressure measurements were made on the centerline of the model access tunnel using a miniaturized, probe-type, pressure gage mount. Side-on and total pressure measurements provide the data required to quantify the pressure regime at these locations within the model. Data analysis indicates that a 1 kg/m^3 increase in loading density produces a corresponding 1.7 MPa increase in overpressure and a 7.2 MPa increase in total pressure within the access tunnel. An analysis is presented in this paper comparing the measured data with theoretical and hydrocode (CTH) calculations.

INTRODUCTION

A considerable amount of research has been performed in the last three decades to develop a data base and prediction methods for airblast from accidental explosions in underground magazines. The airblast measurements recorded were almost exclusively overpressure (side-on). Few attempts were made to measure dynamic flow properties of the blast wave in the tunnel system. During the recently completed Joint US/ROK R&D program for New Underground Ammunition Storage Technologies, an attempt was made to record total pressure waveforms along with the associated overpressure-time histories. The detonations for these experiments entrained large quantities of fine dust in the blast wave which clogged the small vent ports of the total pressure gage mounts, resulting in total pressure waveforms of questionable value.

A program of small-scale, high-explosive airblast experiments was conducted in September 1997 at the WES Big Black Test Site near Vicksburg, MS to evaluate the dynamic flow parameters produced by confined detonations. The program consisted of six experiments using spherical C-4 explosive charges. Total pressures were measured at two locations within the vent pipe using a WES-designed miniature total pressure gage

mount. The experimental program was coupled with hydrocode calculations which allowed a comprehensive analysis of flow conditions in the model.

OBJECTIVE

The overall objective of this research was to quantify dynamic flow parameters from confined detonations. Specific objectives of the research program were to evaluate the effects of explosive loading density (mass of explosive per cubic meter of chamber volume), charge geometry (spherical and rectilinear), and to characterize the dynamic flow parameters of the blast wave.

PHYSICAL MODEL

The airblast experiments were conducted with the steel detonation chamber and pipe originally constructed for Phase 2 of the US/ROK Program, which involved an extensive series of small-scale magazine tests (Joachim, 1994). The model consisted of a detonation chamber connected to a 4-m-long coaxial vent pipe section (see Figure 1). The detonation chamber is cylindrical, with an inside diameter of 508 mm (20 in.) and a length of 1.8 m (5.9 ft), with 152.4-mm (6-in.) thick walls. The vent pipe consisted of four one-meter long sections of 364 mm (14.3 in.) inside diameter Schedule 80 steel pipe. The chamber was sealed with a 76.2 mm (3 in.) steel back plate. The model storage chamber has a cross-sectional area of 0.2027 m^2 and a volume of 0.3649 m^3. The vent pipe cross-sectional area was 0.1038 m^2 and the volume was 0.4152 m^3. The total volume of the model storage magazine was 0.7800 m.

The airblast instrumentation consisted of three side-on pressure gages in the chamber, five side-on and two total pressure gages in the vent pipe, and four side-on pressure gages in the free-field beyond the exit of the vent pipe. Gage locations are shown in Figure 1 and listed in Table 1. Experimental parameters (charge mass and chamber loading density) are given in Table 2. Two WES-designed probe mounts were positioned inside the vent pipe. Each probe mount contained two pressure transducers: a total pressure gage at the front of the probe (oriented face-on to the shock wave), and a side-on gage located in a small chamber 70 mm behind the total pressure gage. The probe side-on pressure gage sensor measured the pressure in an arched chamber of volume of 10,700 mm^3. Pressure entered the chamber through two rows of 1.6-mm-diameter holes drilled at 10^o intervals. A schematic showing the position of the probe mount within a section of vent pipe is shown in Figure 2.

The internal side-on pressure gages were mounted flush with the inside surface of the chamber and vent pipe (except the two gages in the probe mounts). The free-field gages were placed in a surface gage mount such that the gage sensing surface was flush with the ground surface.

EXPLOSIVE CHARGES

Six experiments were conducted in the small-scale magazine using spherical C-4 charges. The masses of the explosive charges used for these experiments were 0.045,

0.28, 0.11 (three experiments), and 1.36 kg. The charges were formed using a hemispherical mold. A Reynolds RP-82 electric bridge wire (EBW) detonator was positioned at the center of the diametrical plane of one hemisphere prior to putting the two hemispherical sections together to form the spherical charge. The charges were suspended at the center of the test chamber using a section of panty-hose and nylon fish line.

COMPUTER MODEL

The computer calculations were performed using CTH, a family of codes developed at Sandia National Laboratories for modeling problems characterized by large deformations or strong shocks (see McGaun, et.al., 1990, and Hertel, et.al, 1993). CTH uses an Eulerian mesh to solve the mass, momentum, and energy conservation equations. The mesh is fixed in space, and the material flows through the mesh in response to boundary and initial conditions. The mesh consists of computational cells, each of which can contain multiple materials and voids.

The scaling relation between the experimental model and prototype magazine was developed as follows. The access tunnel in the prototype was assumed to have a rectangular cross-section, 5-m wide by 5 m in height. Assuming an equivalent circular cross-section, the equivalent diameter was computed to be 5.64 m. The diameter of the access tunnel in the small-scale model was 0.364 m. Therefore, the geometric scale factor relating model and prototype is the ratio of the access tunnel diameters (5.64/0.364 = 15.52). For a chamber loading density of 1.028 kg/m^3 and a charge mass in the model of 0.28 kg of C-4, the charge mass of C-4 in the prototype computes to be 1047 kg. The dimensions of the small-scale model were scaled to the prototype by multiplying by the scale factor (15.52). At a model scale of 15.52, the experimental model represented a prototype chamber 7.88 m in diameter and 27.9 m long, with a volume of 1364 m^3. For the calculations a grid was superimposed on the prototype magazine (25 mm square cells) and the dimensions of the prototype were adjusted to make grid boundaries coincide with cell boundaries. The prototype calculation contained a total of 1,131,900 cells. After gridding the prototype for the CTH calculation, the actual charge mass used in the calculation became 1049 kg of C-4.

The prototype underground magazine was numerically modeled as an axisymmetric geometry. The computational model included three materials; i.e., C-4 explosive, steel, and air. The SNL-SESAME tabular equations-of-state were used to define the properties of the air and steel materials throughout the CTH computations. The C-4 equation-of-state properties were obtained from interpolation of the JWL tables in CTH. A graph of the initial state (before charge detonation) of the axisymmetric computational model is shown in Figure 3. The X coordinate axis is the axis of symmetry for the calculation.

RESULTS AND ANALYSIS

PRESSURE

Measured peak pressure data are plotted versus distance from the center of the explosive charge in Figures 4 through 7. The peak data from a 0.045 kg spherical C-4 detonation are plotted in Figure 4. Least-square curves have been fit to the internal and free-field data. As shown in Figure 4, the probe side-on peak data (square symbol) plots below the trend for the internal (wall of vent pipe) side-on pressure (least-squares data fit curve). The gage baffle apparently reduced the measured peak value. The peak total pressure (diamond symbol) measured at the front of the probe mount is also presented in Figure 4. The peak total pressure is approximately 1.6 times greater than the side-on pressure curve (least-squares fit).

Peak pressure data from three 0.11 kg C-4 experiments are presented in Figure 5. Although the internal gages exhibit some scatter of the peak data, the trend is similar to that shown for the 0.045 kg experiment (Figure 4). The free-field peak pressure data exhibit good repeatability with a low degree of scatter. The peak total pressure values are approximately 2.5 times greater than the side-on pressure curve (least-squares data fit).

Figure 6 presents a plot of peak pressure data from a 0.28 kg spherical C-4 detonation in the small-scale magazine. Here again, the probe mounted side-on pressure gages recorded slightly lower values than were recorded by the side-on pressure gages in the vent tube. The peak total pressure values are approximately three times greater than the side-on pressure curve (least-squares data fit).

A comparison between spherical and rectangular parallelepiped charge geometries is presented in Figure 7. A 1.36 kg rectangular charge (length/diameter ratio = 3) of C-4 was used in the US/ROK small-scale experiments. As shown in Figure 7, data from the two charge geometries plot within normal measurement scatter and are essentially equal. The side-on pressure recorded by gages inside the probe mount cannot be differentiated from the side-on peak data measured at the wall of the vent tube from this experiment.

The stagnation pressure values in Figure 7 recorded from the US/ROK experiment are less than the total pressure data measured with the probe mounts. The stagnation gages were placed 12.7 mm in front of a 25.4 mm steel cube welded to the inside wall of the vent tube. The measured stagnation pressures were apparently influenced by wall turbulence and drag which reduced the peak values. The peak total pressure values at the center of the vent tube are approximately five times greater than the side-on pressure curve (least-squares data fit).

IMPULSE

Pressure waveforms were numerically integrated to obtain impulse-time histories. Peak impulse data from the 0.045 kg experiment are plotted versus distance from the center of the spherical charge in Figure 8. As shown in Figure 8, the impulse data from

the probe mounted side-on pressure gages behind the baffle are indistinguishable from the impulse values measured at the vent tube side-on pressure gages. The values of the impulse lost through the baffle reduction of the peak pressure is very small compared to the total impulse and does not significantly affect the peak side-on impulse values. The total impulse values are approximately 1.7 time greater than the side-on impulse curve (least-squares data fit).

Peak impulse data from three 0.11 kg spherical C-4 detonations are plotted in Figure 9. Although these data exhibit some scatter, the data falls within normal bounds for typical experimental data. The total pressure impulse is approximately 1.7 times greater than the side-on impulse curve (least-squares data fit). A similar comparison is seem in Figure 10 from the 0.28 kg C-4 detonation with a total pressure impulse to side-on pressure impulse ratio of approximately 1.7.

A comparison of impulse data produced by spherical and rectangular parallelepiped charge geometries is presented in Figure 11. A 1.36 kg C-4 charge experiment was conducted in the US/ROK R&D Program small-scale experiments using a rectangular charge. As shown in Figure 11, internal impulse data produced by the two charge geometries plot within normal measurement scatter and are essentially equal. The side-on peak impulse values from gages inside the probe mount cannot be differentiated from the vent tube side-on peak data. The external impulse data from the US/ROK experiment attenuate much faster than the spherical charge impulse data. This is attributed to a difference in the experimental setup. The portal of the model used for the US/ROK experiment vented onto a platform (0.61 m in the axial direction by 0.91 m wide) that was connected to a sloped section to the ground surface. Therefore, the increased attenuation of the free-field impulse values is attributed to the presence of the descending sloped section. The total pressure impulse is approximately 1.7 times the side-on impulse curve (least-squares data fit).

LOADING DENSITY

Peak pressure data are plotted versus loading density in Figure 12. Loading density is the total volume to the gage position divided by the net explosive mass. The total volume includes the volume of the detonation chamber and the vent tube to the measurement point. A least-squares curve has been fit to all the side-on pressure data (spherical and rectangular charges). The slope of the total pressure curve is a factor of 4 times the slope of the side-on pressure curve.

Peak airblast impulse data are plotted versus loading density in Figure 13. A least-squares curve has been fit to all the side-on impulse data (spherical and rectangular charges). The slope of the total pressure impulse curve is a factor of 2 times the slope of the side-on impulse curve.

CALCULATION

A comparison of the measured side-on pressure waveform (Gage AB-5 in the model) scaled up by the scale factor (1:15.52-scale) to the full-scale calculation is presented in Figure 14. As shown here, there is a very good comparison in arrival times of the various portions of the waveform. The major difference is the second peak of the calculations associated with the reflection off the rear wall of the detonation chamber. The calculated peak is approximately twice the measured value. It is postulated that the reflecting surface is much stiffer in the calculational model than it was in the small-scale physical model.

A comparison of three calculated waveforms, i.e., side-on, dynamic, and total pressure, is shown in Figure 15. The CTH computer code calculated the side-on pressure waveform directly. The code also calculated air density and particle velocity waveforms for each gage location. Since these waveforms had the same time values, it is a simple matter to derive the dynamic pressure waveform using the equation:

$$P_{dyn} = 1/2\, r\, u^2 \qquad \textbf{(1)}$$

where P_{dyn} is the dynamic pressure component at each time increment,
ρ is the air density component at each time increment,
and u is the particle velocity component.

The total pressure waveform was computed with a spread sheet using the relation:

$$P_t = P_{dyn} + P_{so} \qquad \textbf{(2)}$$

where P_t is the total pressure component at each time increment,
and P_{so} is the side-on pressure component.

Figure 15 compares calculated waveforms for the gage location in the full-scale computational model corresponding to Gage AB-7 in the physical model (small-scale).

A comparison of the calculated full-scale total pressure waveform and scaled up measured waveform from the physical model is presented in Figure 16. The small-scale data are scaled up to full-scale by multiplying the time by the scale factor (15.52). The waveforms are in excellent agreement, except for the reflected peak value where the calculated peak is more than twice the measured value.

An overpressure waveform comparison at a full-scale distance of 38.3 m from the center of the explosive charge is shown in Figure 17. This location corresponds to Gage AB-6 in the physical model. The measured and calculated waveforms are in relatively good agreement. The measured waveform does not have the rapid rise time seen in the calculation because this gage was located behind a baffle on the side of the total pressure probe behind a baffle. A CONWEP-calculated (Hyde, 1988), full-scale, free-field overpressure waveform is included in Figure 17 for additional comparison. This comparison emphasizes how the confinement of the chamber and tunnel increases the

pressure at a given range compared to the free-field pressure at the same range from an unconfined detonation.

In Figure 18, the total airblast impulse and the overpressure impulse waveforms in the confined space of the underground magazine facility are compared to the calculated (CONWEP, Hyde, 1988) impulse waveform in the free-field at the same distance from an unconfined detonation. Note the dramatic increase in impulse resulting from confinement. The peak total calculated impulse is a factor of 1.5 greater than the peak side-on (measured overpressure) impulse at this location.

Calculated waveforms on the centerline of the access tunnel at 52.8 m (full-scale) from the center of the explosive charge are shown in Figure 19. This location corresponds to the position of Gage AB-9 in the small-scale experiments. The CTH code was used to calculate the side-on pressure waveform, air density, and particle velocity waveforms at this position in the tunnel. The dynamic pressure waveform was computed using Equation 1. The sum of the side-on and dynamic pressure waveforms yields the total pressure waveform (Equation 2).

A comparison of the calculated full-scale total pressure waveform (from Figure 19) and the scaled-up measured waveform from the physical model is presented in Figure 20. The waveforms are in good agreement. The calculated waveform does not exhibit the excessive reflected peak seen in previous waveform comparisons.

An overpressure waveform comparison at a full-scale distance of 53.9 m from the center of the explosive charge is shown in Figure 21. This location corresponds to Gage AB-8 in the physical model. The measured and calculated waveforms are in relatively good agreement. The measured waveform does not have the rapid rise time seen in the calculation because this gage was also located on the side of the total pressure probe behind a baffle. A full-scale free-field overpressure waveform is calculated using CONWEP is included for an additional comparison.

In Figure 22, the total airblast impulse and overpressure impulse waveforms in the confined space of the underground facility are again compared to the free-field impulse waveform from CONWEP at the same distance from an unconfined detonation. Note the dramatic increase in impulse resulting from the confinement. The calculated peak total impulse is a factor of 1.7 greater than the peak side-on impulse (from the measured overpressure) at this location.

A plot of peak overpressure versus distance from the rear wall of the detonation chamber is shown in Figure 23. Overpressures were calculated on the centerline and side wall throughout the chamber/tunnel facility. The measured peak overpressure data (scaled up) are plotted in Figure 23 for comparison. The measured data are a factor of 2 or more less than the calculated (wall) curve. As was shown in Figures 14 -17, 19 and 21, the larger calculated peak overpressure values are due to the reflected (second) peak found in these waveforms.

CONCLUSIONS

Comparisons of the CTH full-scale and scaled up small-scale measured overpressure show excellent agreement. A total pressure waveform was computed using the CTH calculated side-on pressure, air density, and particle velocity waveforms. The computed full-scale total pressure show excellent agreement with the scaled up measured total pressure waveform from the small-scale (1:15.52-scale) experiments.

Comparison of airblast pressures generated by the detonation of 1.36 kg C-4 spherical and rectangular (length/diameter ratio = 3) C-4 charges in the small-scale magazine show that differences in measured peak pressures values fall within normal bounds for gas/shock pressure measurement. Similarly, comparisons of peak impulse values derived from these experiments show no significant difference between the impulse data from these experiments.

Confinement in an underground facility dramatically increases the amplitudes of pressure and impulse waveforms over those generated by detonations in the free-field. Comparisons show that the internal pressure and impulse waveforms are orders of magnitude greater than the free-field values for equal yield and distance.

Analysis of the data presented herein indicates that a 1 kg/m^3 increase in loading density produces a corresponding 1.7 MPa (approximately) increase in overpressure and a 7.2 MPa increase in total pressure within the access tunnel. Similarly, a 1 kg/m^3 increase in loading density produces a corresponding 4.7 MPa-sec increase in side-on pressure impulse and a 9.3 MPa-sec increase in total impulse. Total impulse is on the order of 1.5 to 2.0 times the side-on impulse. These observations are limited to the magazine designs and to the range of explosive masses and loading densities used in these experiments.

ACKNOWLEDGEMENTS

We appreciate the cooperation of the authorities at the U.S. Army Engineer Waterways Experiment Station, and the Headquarters, U.S. Army Corps of Engineers that permitted us to prepare and present this paper for publication.

REFERENCES

Hertel, G. I., McGaun, J. M. , Petney, S. V., Silling, S. A., Taylor, P. A., and Yarrington, L., "CTH: A Software Family for Multi-Dimensional Shock Physics Analysis," Proceedings of the 19th International Symposium on Shock Waves, 1993, **1**, 377-382.

Hyde, D. W., "Users Guide for Microcomputer Programs CONWEP and FUNPRO, Applications of TM 5-855-1, Fundamental of Protective Design for Conventional Weapons," Instruction Report SL-88-1, April 1998, U.S. Army Engineer Waterways Experiment Station, Vicksburg, MS.

Joachim. C. E., “Parameter Study for Underground Ammunition Storage Magazines: Results of explosion Tests in Small-Scale Models,” Twenty-Sixth Explosives Safety Seminar, 16-18 August 1994, Miami, FL.

McGlaun, J. M., Thompson, S. L. and Elrick, M. G., “CTH: A Three Dimensional Shock Wave Physics Code,” International Journal of Impact Engineering, 1990, **10**, 351-360.

Table 1. Gage location, model ammunition storage magazine, airblast effects experiments

Gage No.	Distance from Rear Wall of Chamber (m)	Distance from Axis of Chamber/Tunnel (m)	Measurement Location
AB-1	0.00	0.107	Back Wall of Chamber, Chamber Pressure
AB-2	0.45	0.254	Side Wall of Chamber, Chamber Pressure
AB-3	1.35	0.254	Side Wall of Vent Pipe, Side-on Pressure
AB-5	2.61	0.182	Side Wall of Vent Pipe, Side-on Pressure
AB-6	3.37	0.019	Side of Probe Mount, Side-on Pressure
AB-7	3.30	0.000	End of Probe Mount, Total Pressure
AB-8	4.37	0.019	Side of Probe Mount, Side-on Pressure
AB-9	4.30	0.000	End of Probe Mount, Total Pressure
AB-10	5.30	0.182	Side Wall of Vent Pipe, Side-on Pressure
AB-11	5.61	0.182	Side Wall of Vent Pipe, Side-on Pressure
AB-12	7.60	0.182	Free-Field, Side-on Pressure
AB-13	8.80	0.182	Free-Field, Side-on Pressure
AB-15	10.60	0.182	Free-Field, Side-on Pressure
AB-17	13.80	0.182	Free-Field, Side-on Pressure

Table 2. Test parameters of model underground ammunition storage magazine for blast effects experiments

Experiment No.	C-4 Explosive Mass (kg)	Chamber Loading Density (kg/m^3)	Facility Total Loading Density (kg/m^3)
1	0.11	0.404	0.184
2	0.11	0.404	0.184
3	0.11	0.404	0.184
4	0.28	1.028	0.468
5	1.36	4.995	2.273
6	0.045	0.165	0.075
7[1]	1049	1.028	0.468

1 CTH prototype underground ammunition storage magazine computational model

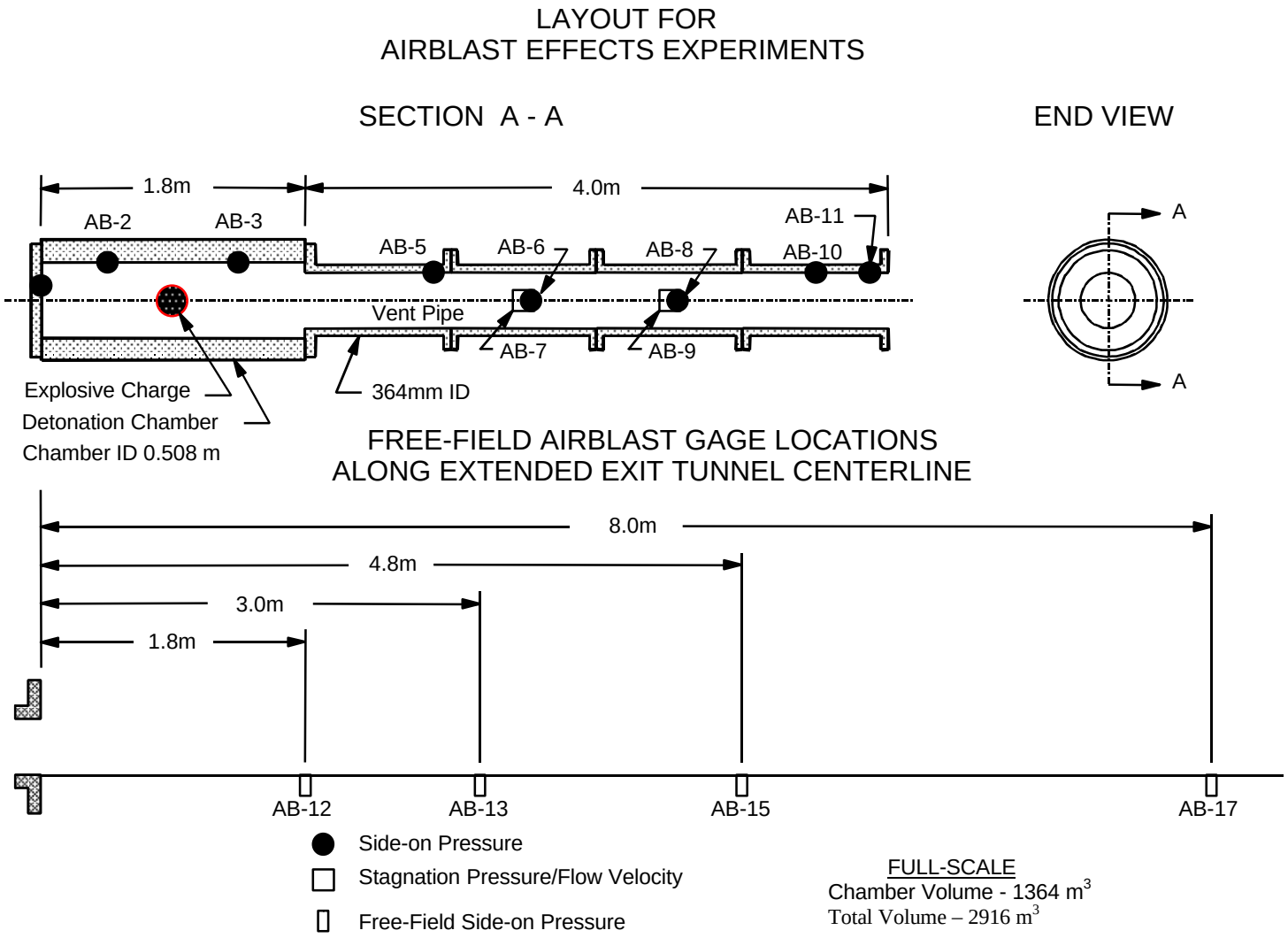

Figure 1. Layout of model underground ammunition storage magazine experiment. Internal and free-field instrumentation type and location are shown.

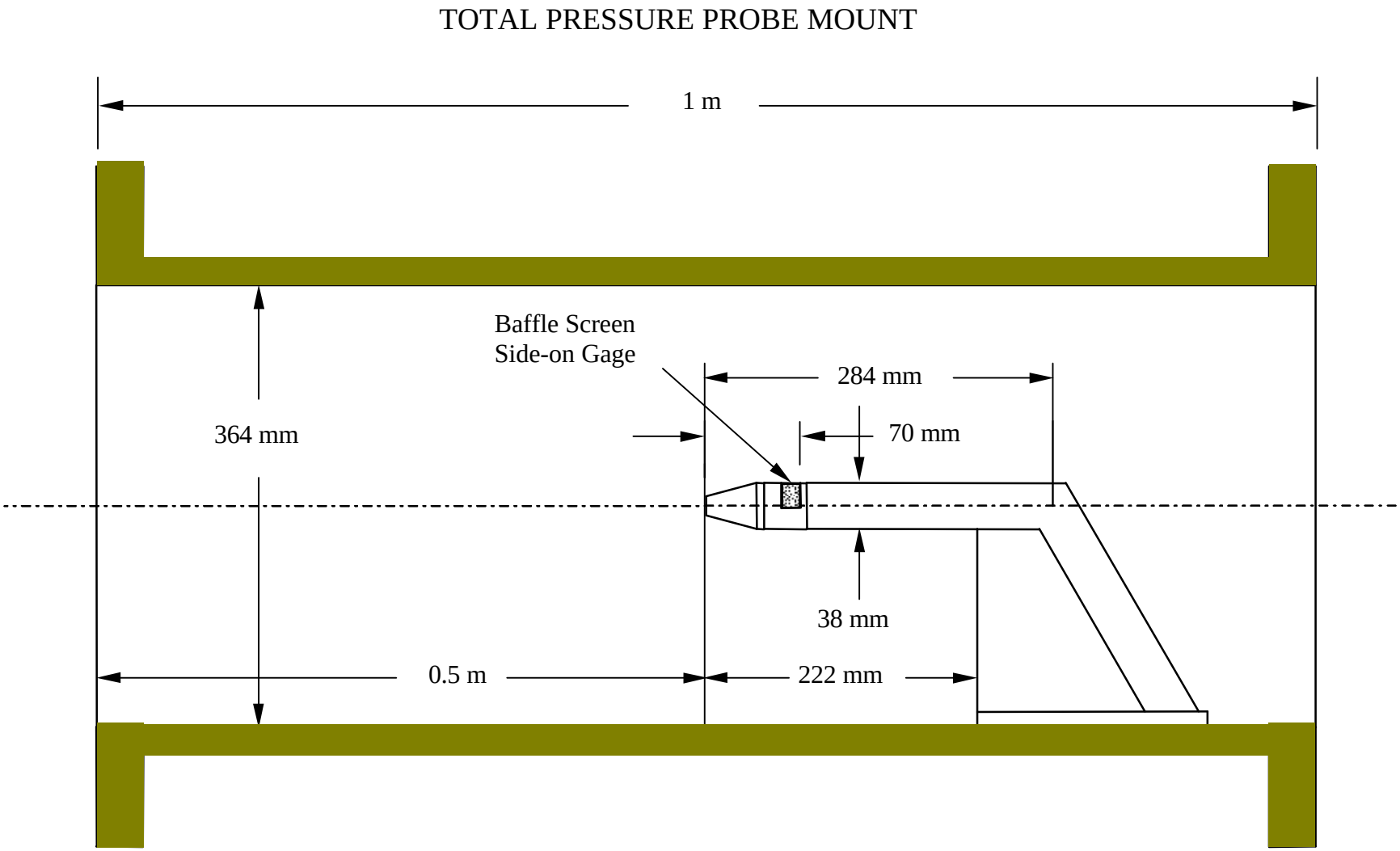

Figure 2. Schematic showing position of total pressure probe mount within the vent pipe and the relative position of side-on pressure blast screen with respect to the total pressure gage.

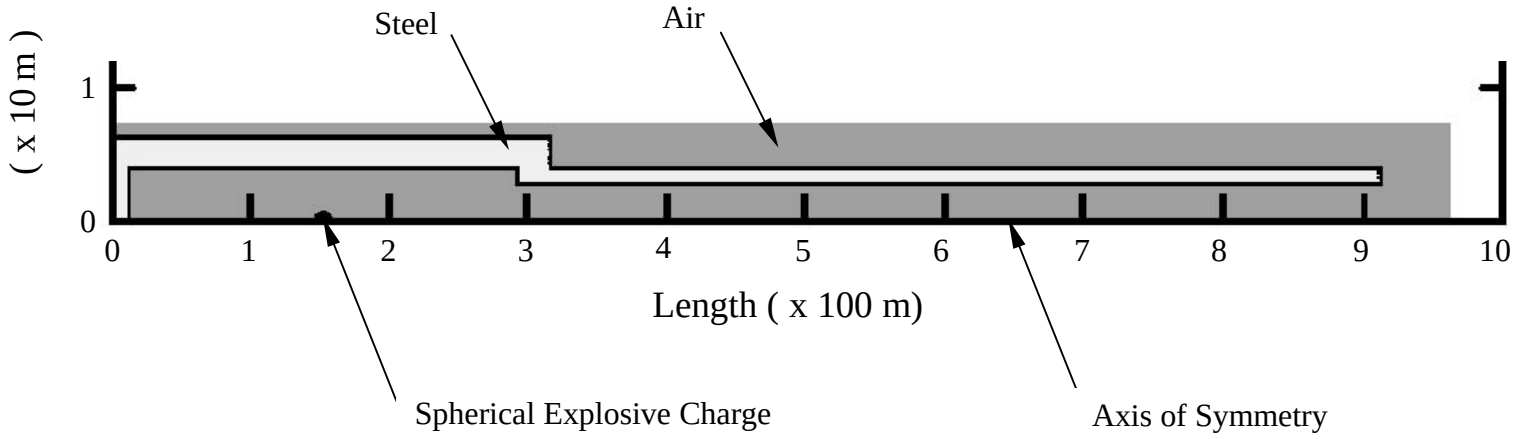

Figure 3. Visual display of prototype magazine computational model for airblast effects study. Note: dark shaded area depicts a diameter of 7.35 m (294 cells) and a length of 96.25 m (3850 cells).

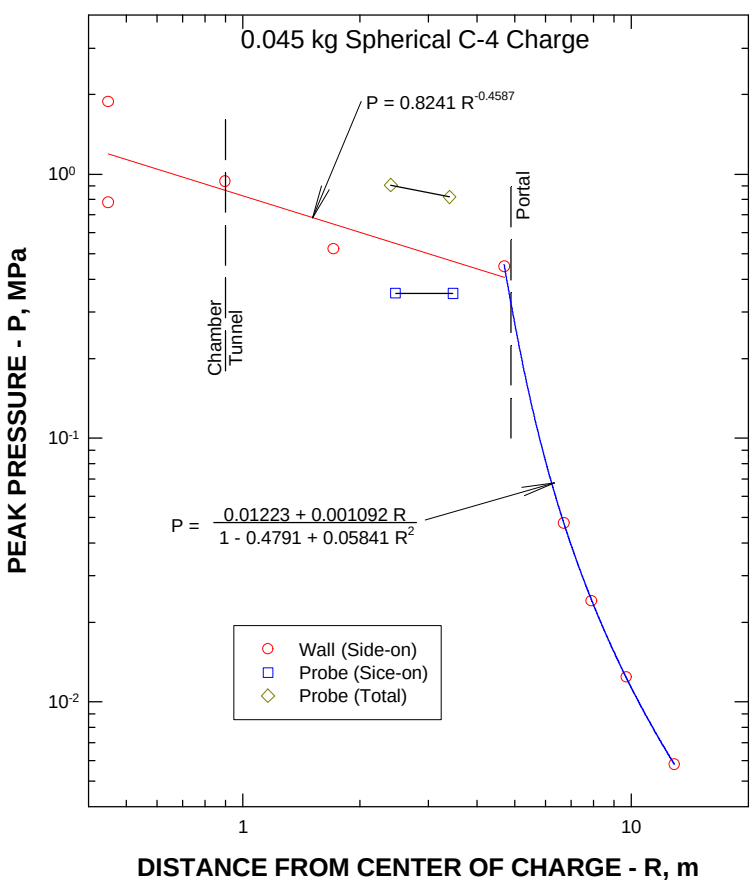

Figure 4. Peak airblast pressure versus distance from the center of the explosive charge for a 0.045 kg spherical C-4 charge detonation, airblast experiments in small-scale magazines.

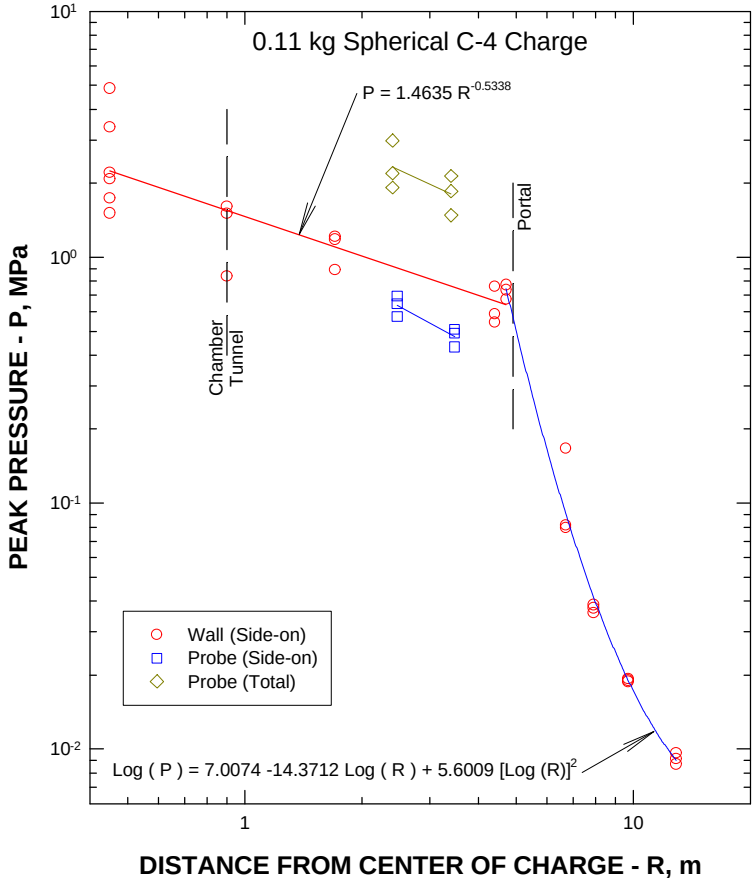

Figure 5. Peak airblast pressure versus distance from center of the explosive charge for a 0.11 kg spherical C-4 charge detonation (three experiments), airblast experiments in small-scale magazines.

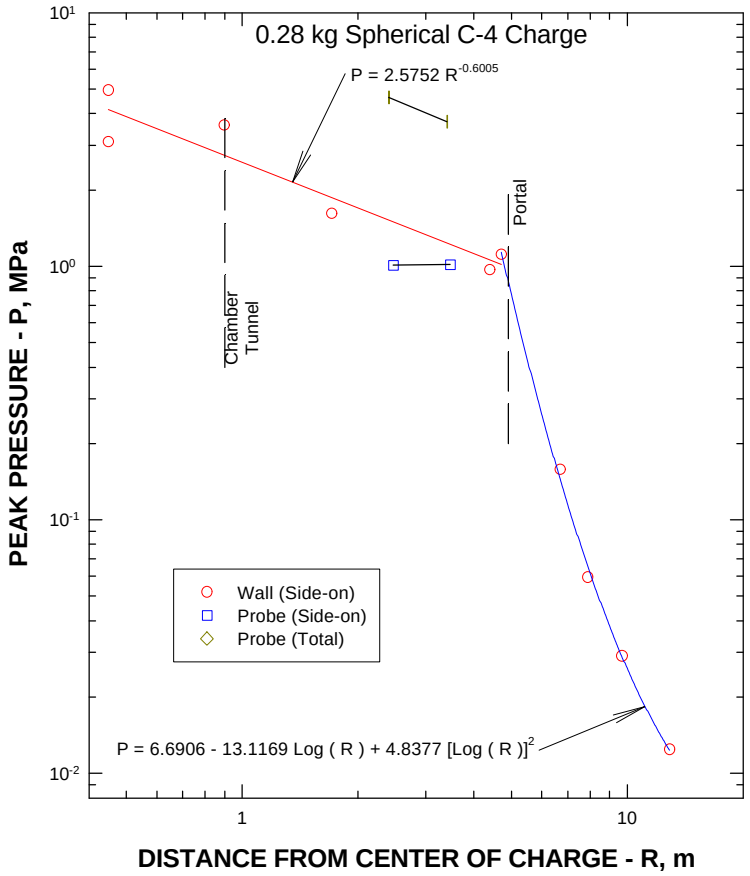

Figure 6. Peak airblast pressure versus distance from the center of the explosive charge for a 0.28 kg spherical C-4 charge detonation, airblast experiments in small-scale magazines.

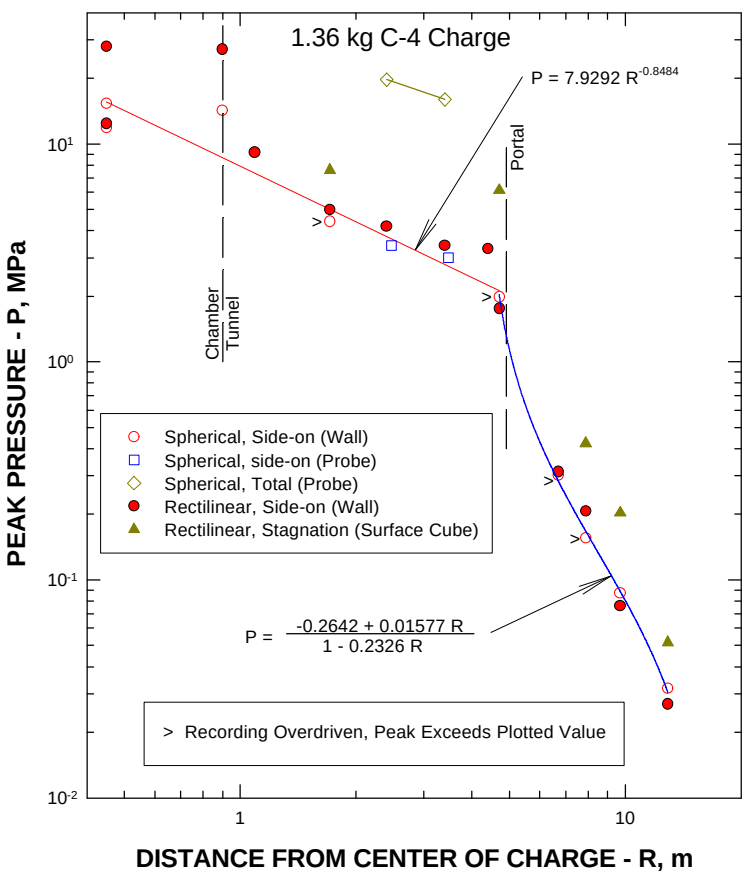

Figure 7. Peak airblast pressure versus distance from the center of the explosive charge for 1.36 kg spherical C-4 detonation, airblast experiments in small-scale magazines. Comparison is shown between peak pressure data from spherical and parallelepiped (rectilinear) charge geometries.

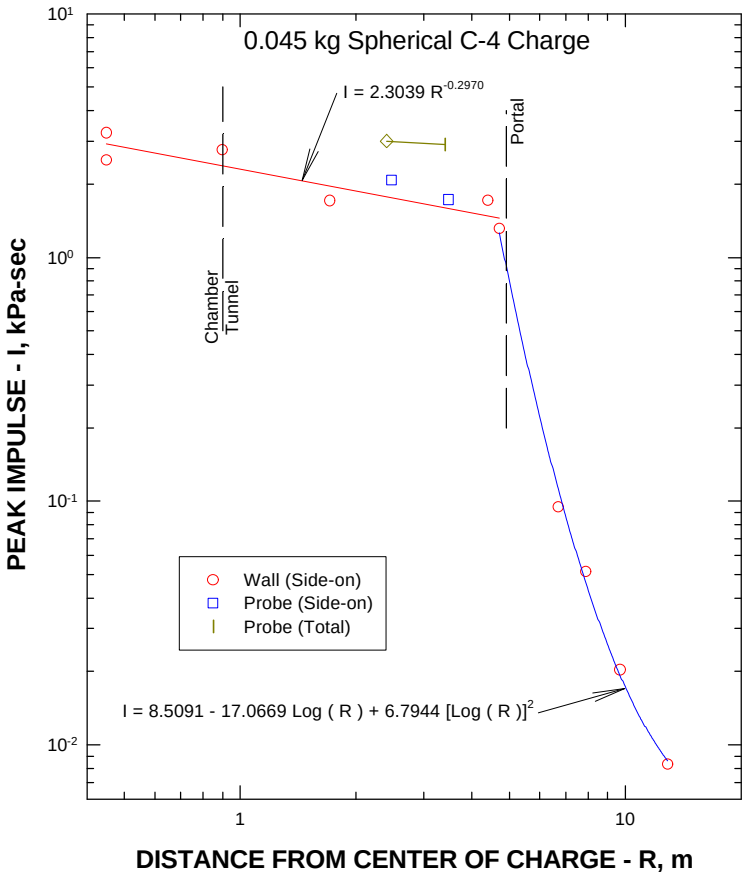

Figure 8. Peak airblast impulse versus distance from the center of the explosive charge for a 0.045 kg spherical C-4 charge detonation, airblast experiments in small-scale magazines.

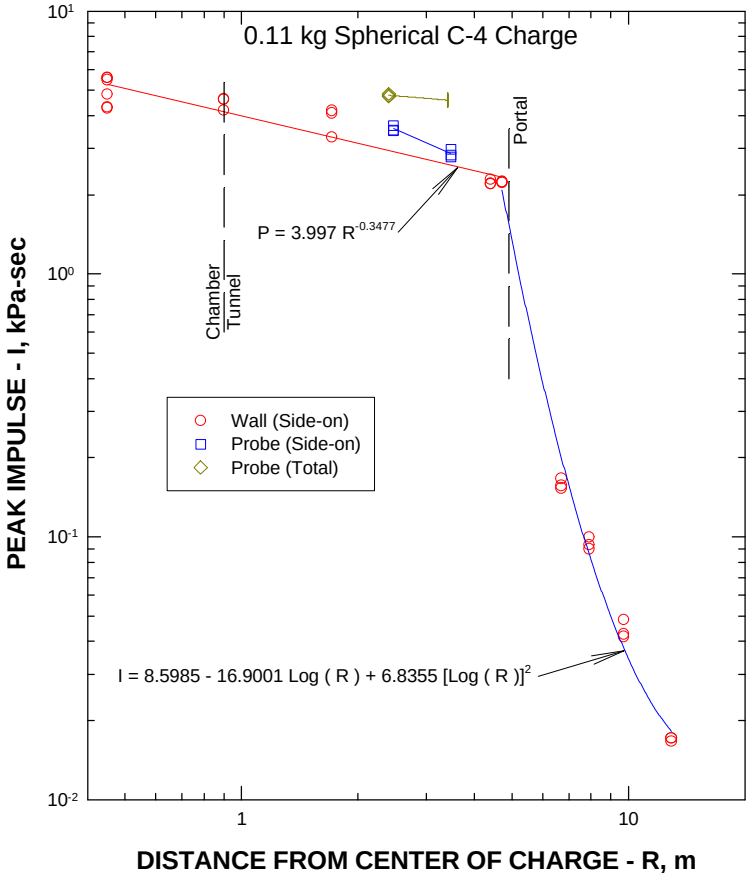

Figure 9. Peak airblast impulse versus distance from center of the explosive charge for a 0.11 kg spherical C-4 charge detonation (three experiments), airblast experiments in small-scale magazines.

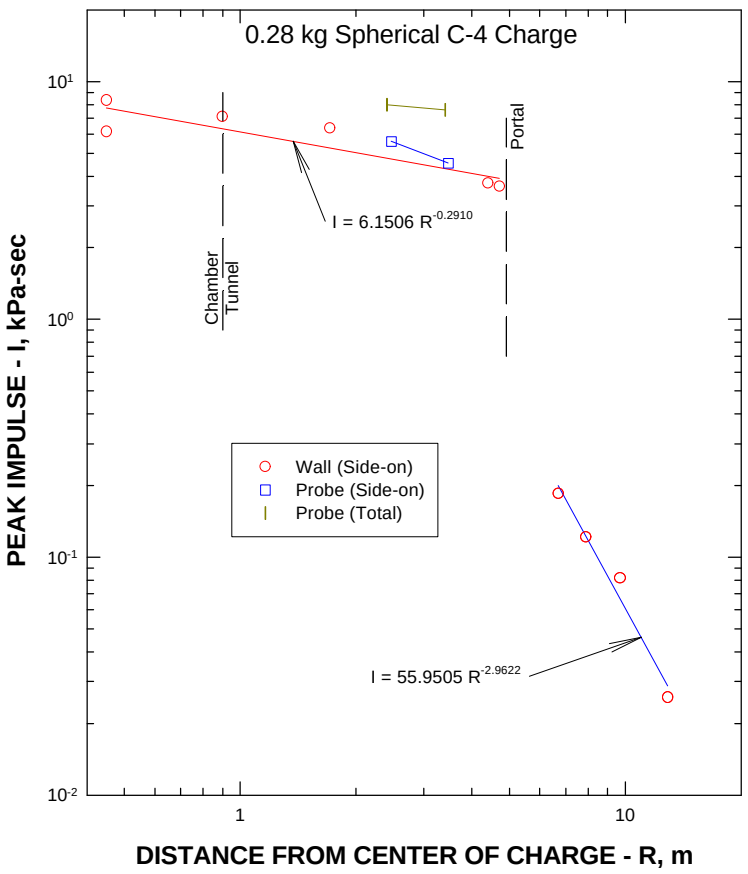

Figure 10. Peak airblast impulse versus distance from the center of the explosive charge for a 0.28 kg spherical C-4 charge detonation, airblast experiments in small-scale magazines.

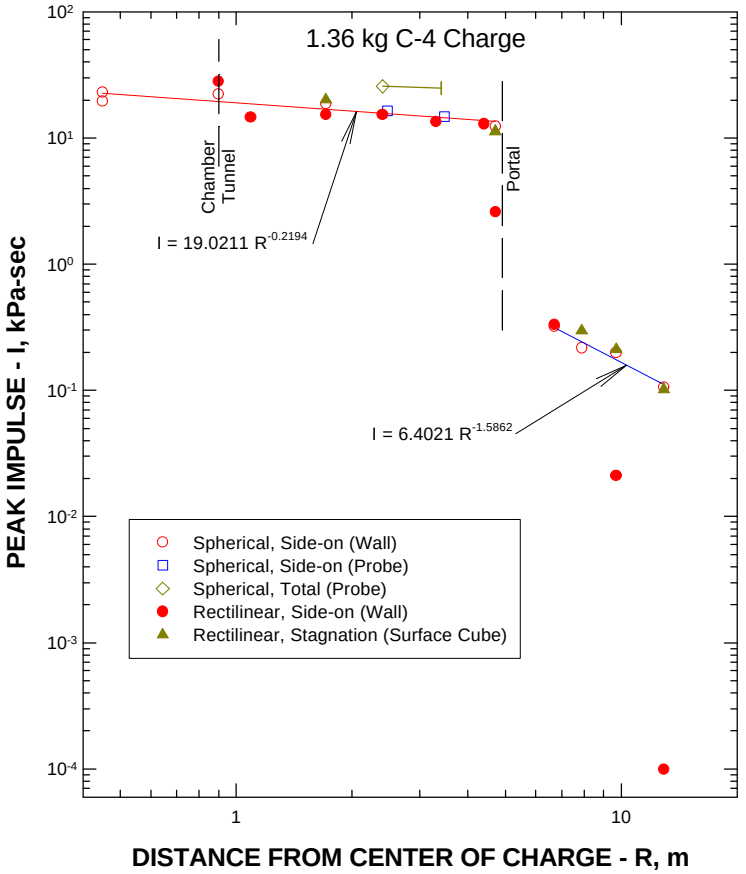

Figure 11. Peak airblast impulse versus distance from the center of the explosive charge for 1.36 kg spherical C-4 detonation, airblast experiments in small-scale magazines. Comparison is shown between peak pressure data from spherical and parallelepiped (rectilinear) charge geometries.

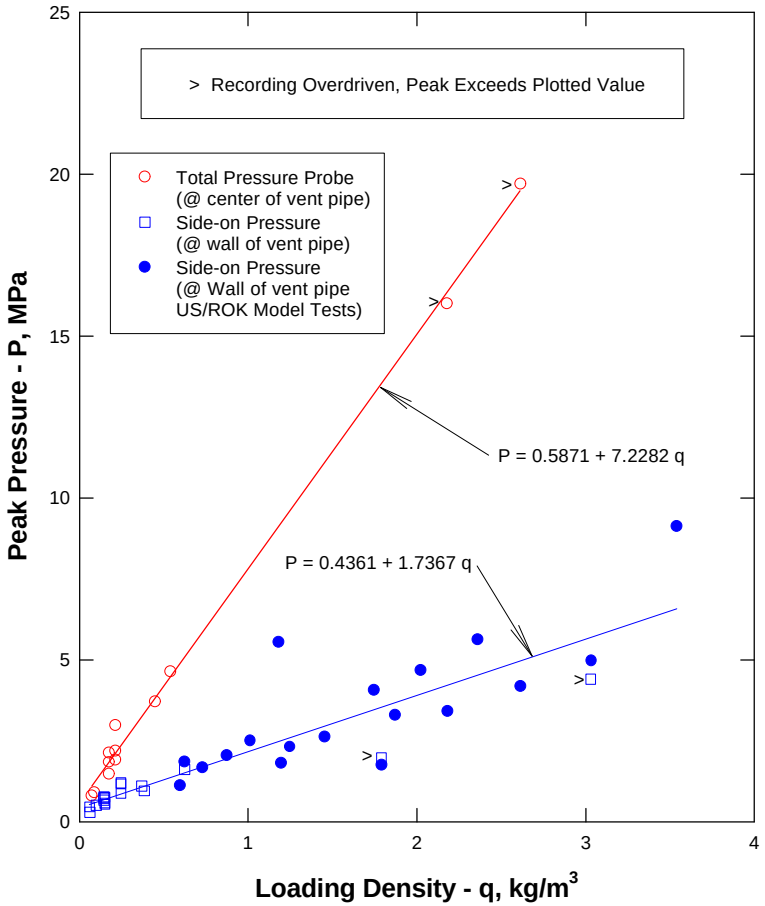

Figure 12. Peak airblast pressure versus explosive loading density, airblast experiments in small-scale magazines. Loading density is the explosive mass divided by the total encompassed volume to the measurement point. Comparison is shown between peak side-on pressure data from spherical and rectangular parallelepiped (US/ROK Program) charge geometries.

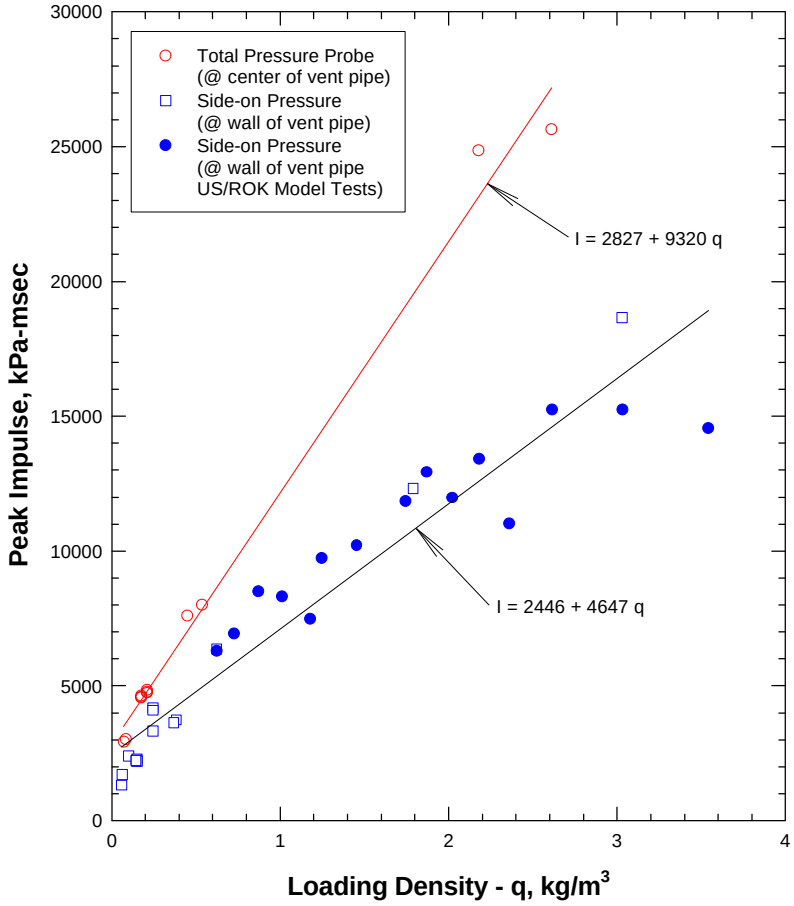

Figure 13. Peak airblast impulse versus explosive loading density, airblast experiments in small-scale magazines. Loading density is the explosive mass divided by the total encompassed volume to the measurement point. Comparison is shown between peak side-on impulse data from spherical and rectangular parallelepiped (US/ROK Program) charge geometries.

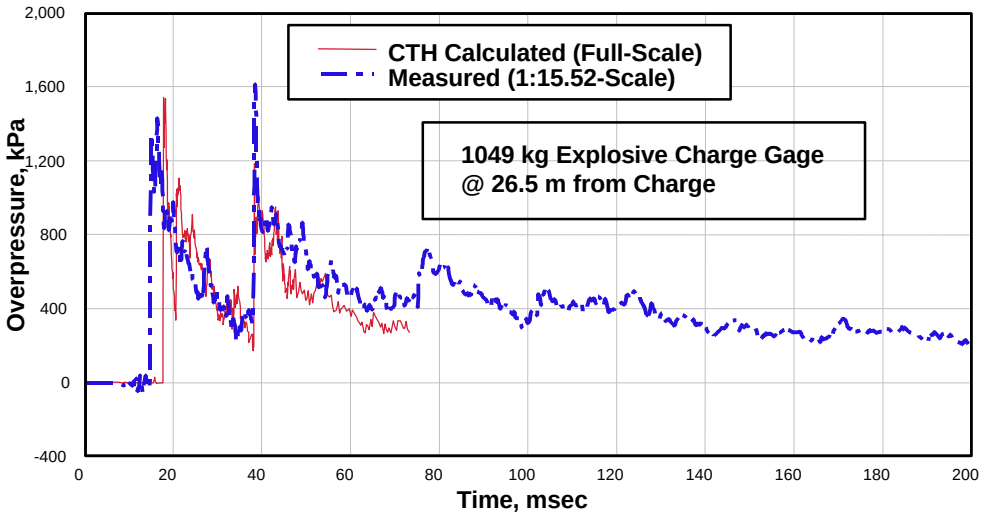

Figure 14. Comparison of measured (1:15.52-scale and calculated (CTH full-scale) overpressure waveforms on the side wall of the exit tunnel at 26.5 m (full-scale) from the center of the explosive charge. The charge was 0.28 kg for the experiment (model) that scaled to 1049 kg in the calculation (full-scale).

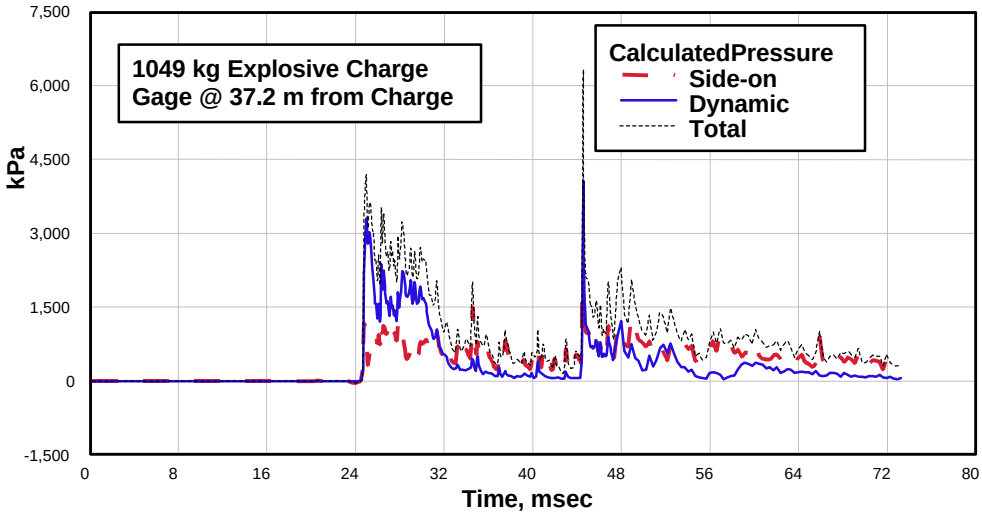

Figure 15. Calculated (CTH) pressure waveform on the centerline of the exit tunnel at 37.2 m from the center of the explosive charge. The calculated overpressure waveform (CTH) is compared with calculated dynamic pressure (Equation 1) and calculated total pressure (Equation 2) waveforms.

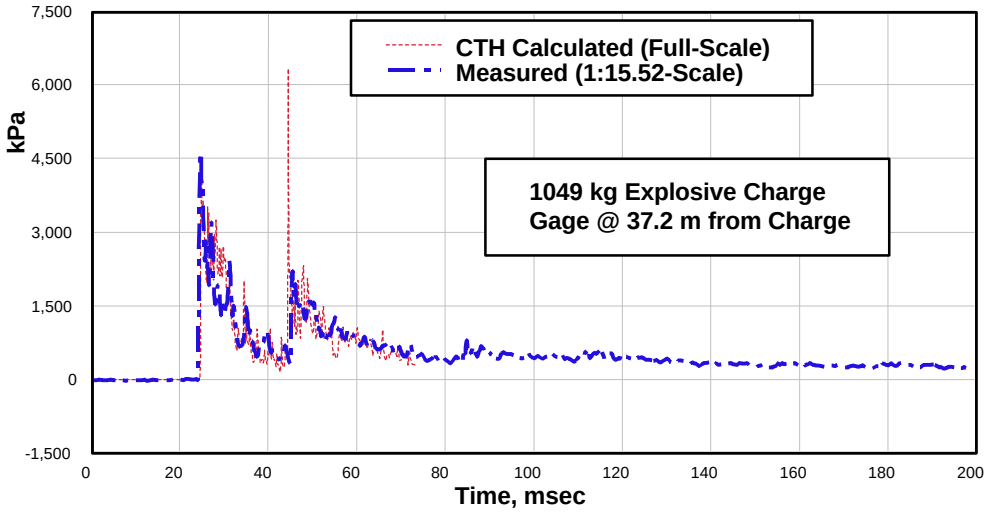

Figure 16. Comparison of measured (1:15.52-scale) and calculated (CTH full-scale) total pressure waveforms on the centerline of the exit tunnel at 37.2 m from the center of the explosive charge. The charge was 0.28 kg for the experiment (model) that scaled to 1049 kg in the calculation (full-scale).

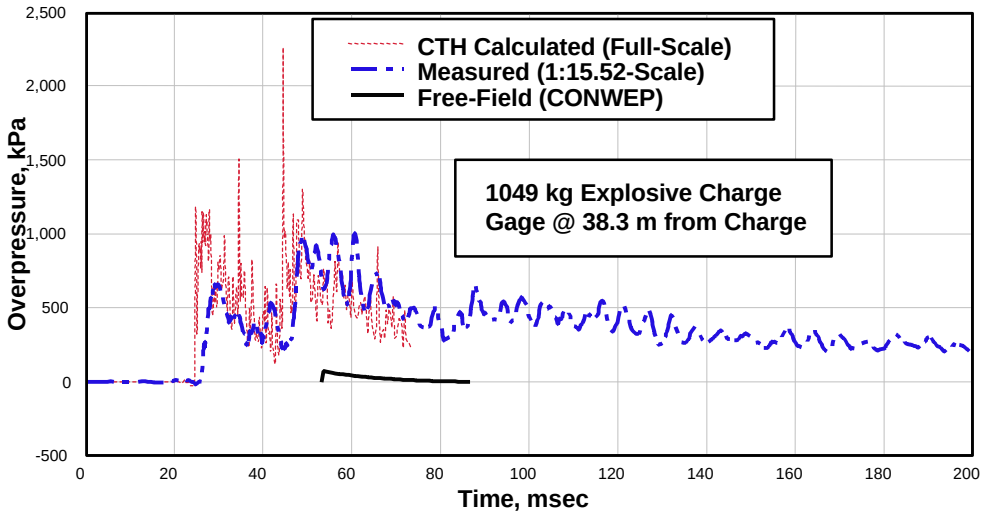

Figure 17. Comparison of measured (1:15.52-scale) and calculated (CTH and CONWEP) full-scale overpressure waveforms on the centerline of the exit tunnel at 38.3 m from the center of the explosive charge. The measured waveform (model) was recorded from a gage located behind a baffle in the side of the total pressure probe mount.

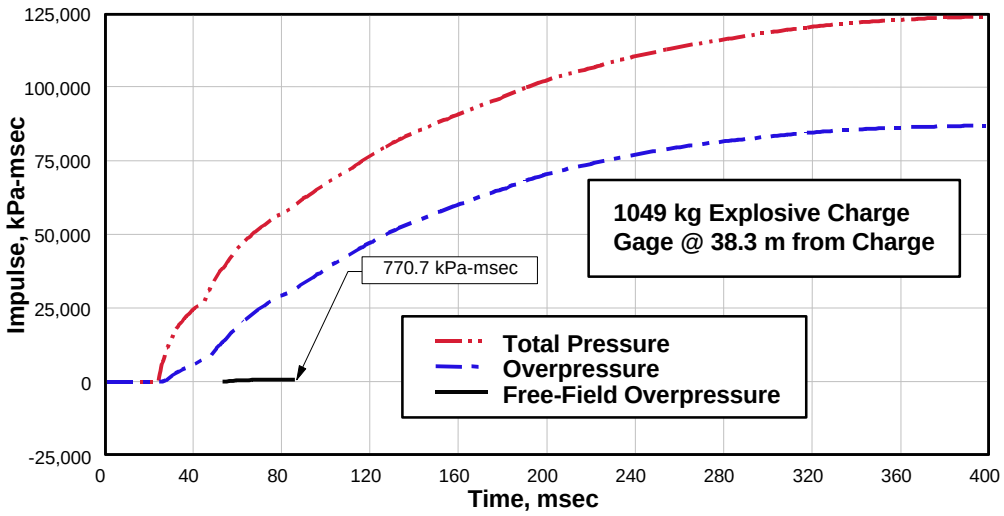

Figure 18. Total and side-on impulse waveforms obtained by integrating the airblast waveforms presented in Figure 15.

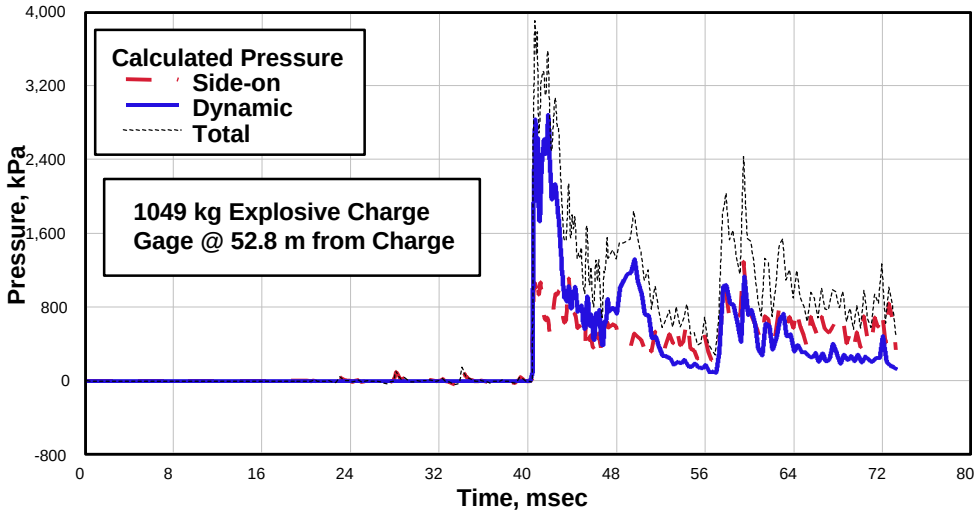

Figure 19. Calculated (CTH) pressure waveforms on the centerline of the exit tunnel at 52.8 m from the center of the explosive charge. Calculated overpressure waveform (CTH) is compared with calculated dynamic pressure (Equation 1) and calculated total pressure (Equation2) waveforms.

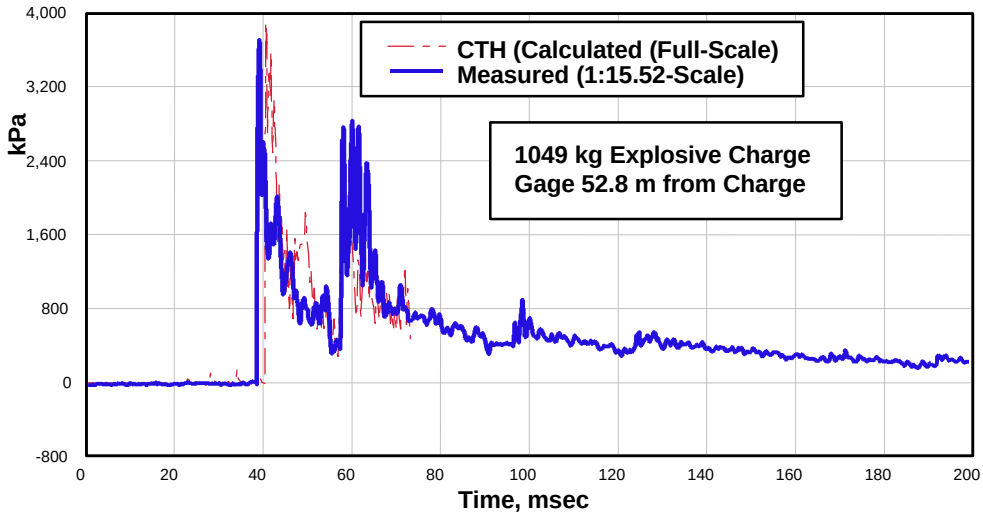

Figure 20. Comparison of measured (1:15.52-scale) and calculated (CTH full-scale) total pressure waveforms on the centerline of the exit tunnel at 52.8 m from the center of the explosive charge. The charge was 0.28 kg for the experiment (model) that scaled to 1049 kg in the calculation (full-scale).

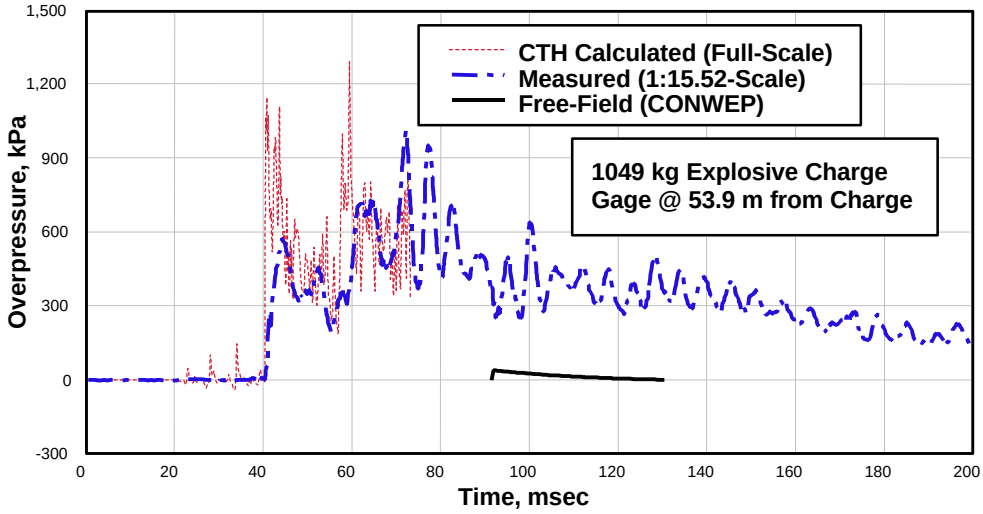

Figure 21. Comparison of measured (1:15.52-scale) and calculated (CTH and CONWEP) full-scale overpressure waveforms on the centerline of the exit tunnel at 53.9 m from the center of the explosive charge. The measured waveform (model) was recorded from a gage located behind a baffle in the side of the total pressure probe mount.

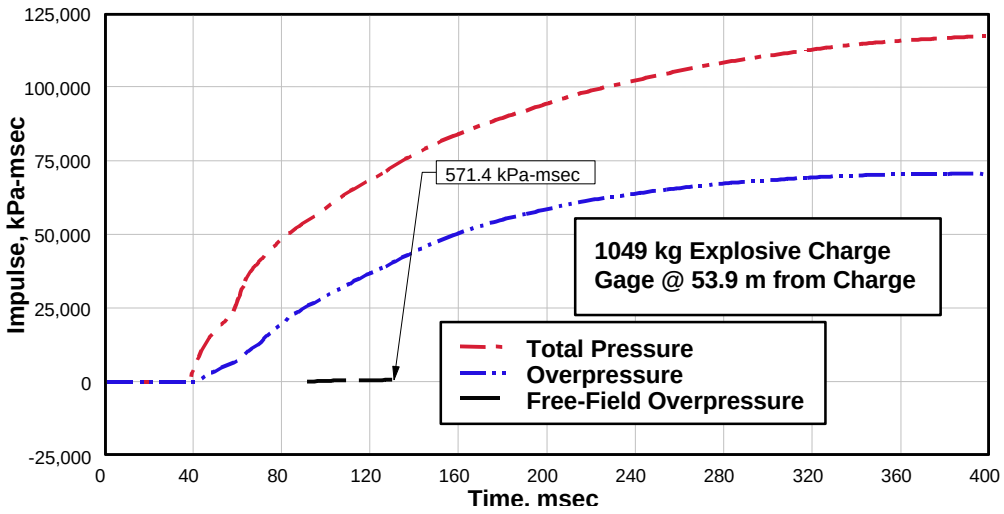

Figure 22. Total and side-on impulse waveforms obtained by integrating the airblast waveforms presented in figure 20.

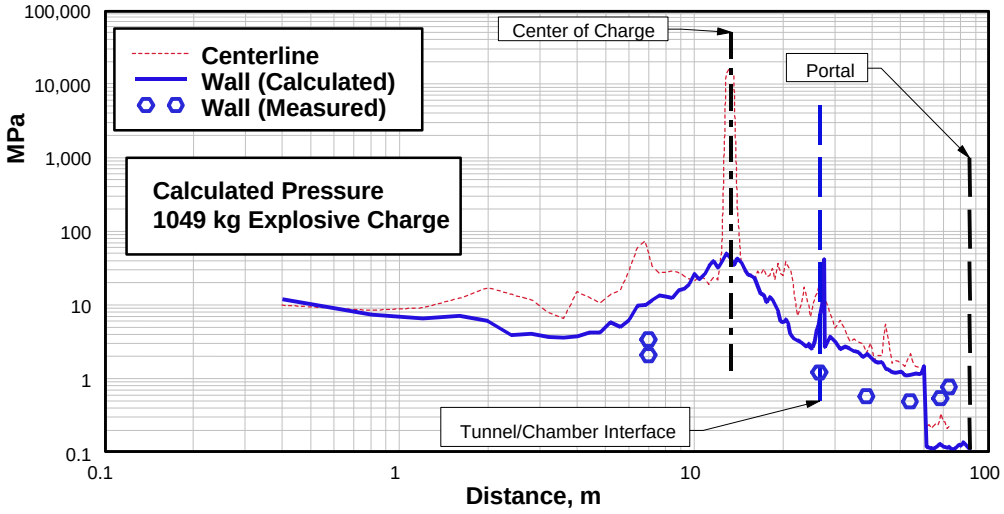

Figure 23. Comparison of peak overpressures along the surface of the wall (1:15.52-scale and full-scale) and centerline (full-scale) of the chamber/tunnel, airblast effects experiments in small-scale vented "shot-gun" magazines.